Supporting Information

Rational design of electrocatalysts for simultaneously promoting bulk charge separation and surface charge transfer in solar water splitting photoelectrodes

Yingfei Hu,[a] Yangqing Wu,[b] Jianyong Feng,[a] Huiting Huang,[a] Chunchen Zhang,[a] Qinfeng Qian,[a] Tao Fang,[a] Jun Xu,[b] Peng Wang,[a] Zhaosheng Li,*[a] and Zhigang Zou[ac]

[a.]Collaborative Innovation Center of Advanced Microstructures, National Laboratory of Solid State Microstructures, College of Engineering and Applied Sciences, Nanjing University, 22 Hankou Road, Nanjing 210093, P. R. China

[b.]School of Electronic Science and Engineering, Nanjing University, 22 Hankou Road, Nanjing 210093, P. R. China

[c.]Jiangsu Key Laboratory for Nano Technology, Nanjing University, 22 Hankou Road, Nanjing 210093, P. R. China

* Corresponding author: Zhaosheng Li

E-mail: zsli@nju.edu.cn (Z. S. Li)

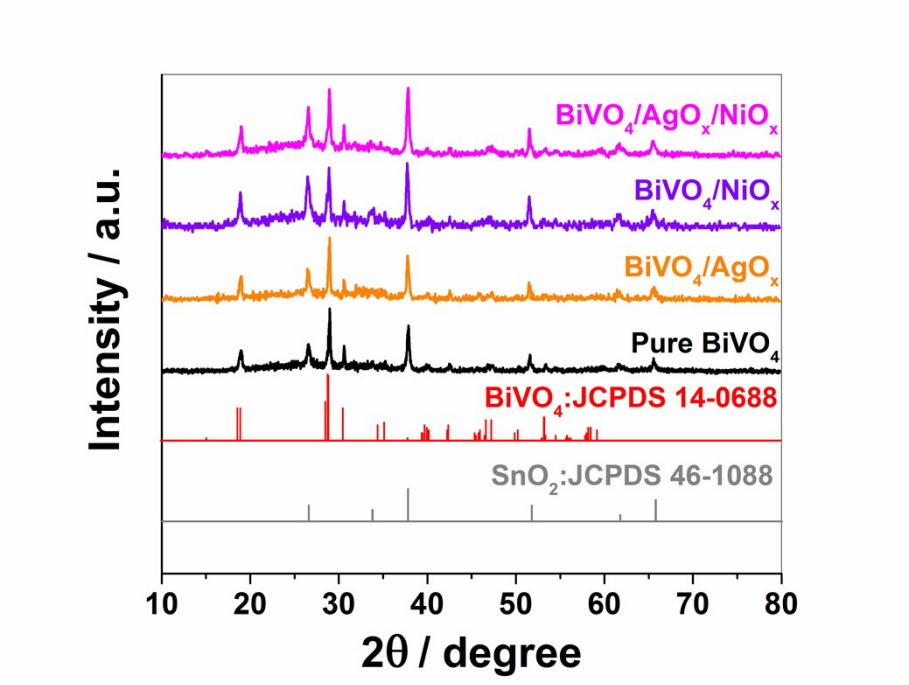

Fig. S1 XRD patterns of the pure $BiVO_4$, $BiVO_4/AgO_x$, $BiVO_4/NiO_x$, and $BiVO_4/AgO_x/NiO_x$ photoanodes.

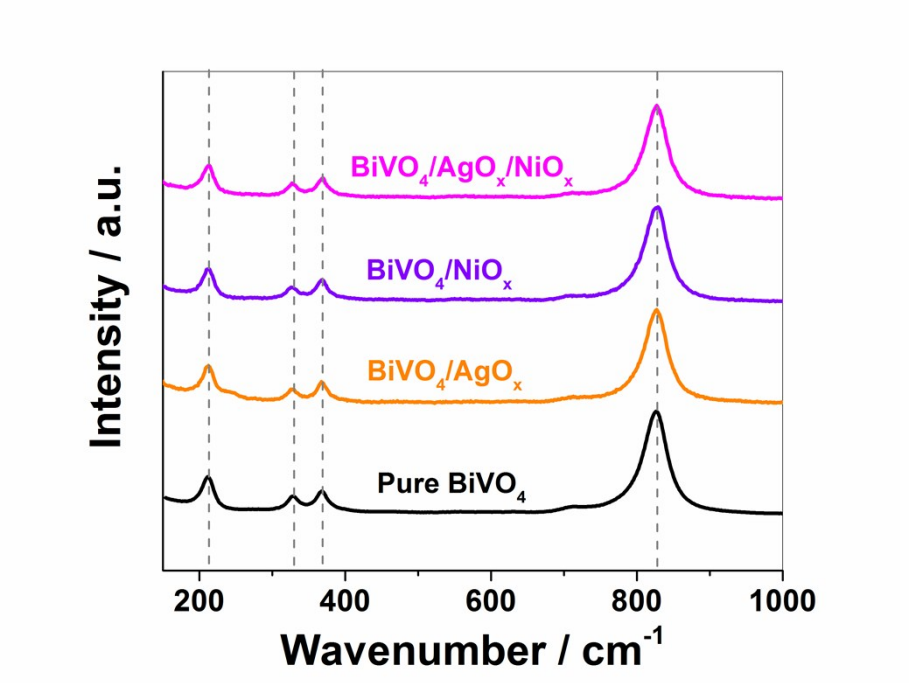

Fig. S2 Raman spectra of the pure $BiVO_4$, $BiVO_4/AgO_x$, $BiVO_4/NiO_x$, and $BiVO_4/AgO_x/NiO_x$ photoanodes.

Table S1. Photocurrents of the pure $BiVO_4$, $BiVO_4/AgO_x$, $BiVO_4/NiO_x$, and $BiVO_4/AgO_x/NiO_x$ photoanodes at 0.60 V_{RHE} and 1.23 V_{RHE}.

Samples / V_{RHE}	$BiVO_4$ (mA/cm^2)	$BiVO_4/AgO_x$ (mA/cm^2)	$BiVO_4/NiO_x$ (mA/cm^2)	$BiVO_4/AgO_x/NiO_x$ (mA/cm^2)
0.6	0.08	0.22	0.61	1.24
1.23	1.14	1.33	1.85	2.25

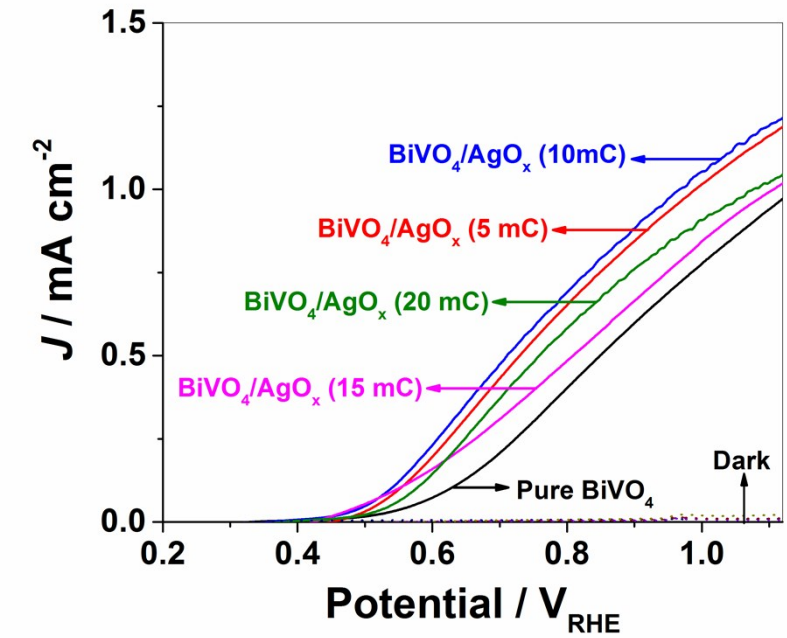

Fig. S3 Photocurrents of the pure $BiVO_4$ (black) and $BiVO_4$ photoanodes deposited by various amounts of AgO_x (5 mC, 10 mC, 15 mC, 20 mC) in 0.2 M KBi (pH = 9.25) electrolyte under AM 1.5 G 100 mW cm^{-2} simulated sunlight.

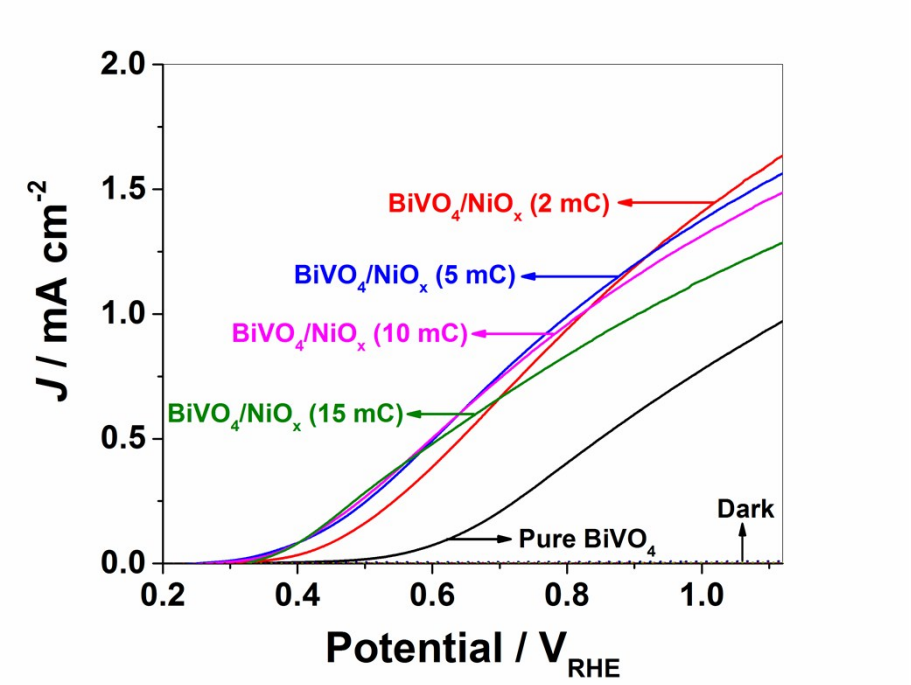

Fig. S4 Photocurrents of the pure $BiVO_4$ (black) and $BiVO_4$ photoanodes deposited by various amounts of NiO_x (2 mC, 5 mC, 10 mC, 15 mC) in 0.2 M KBi (pH = 9.25) electrolyte under AM 1.5 G 100 mW cm^{-2} simulated sunlight.

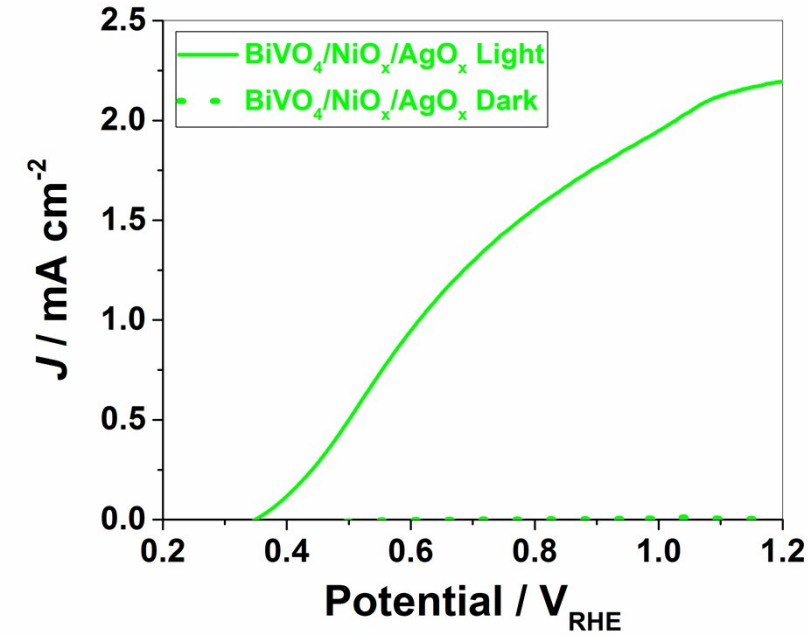

Fig. S5 The photocurrent of the $BiVO_4/NiO_x/AgO_x$ photoanode in 0.2 M KBi (pH = 9.25) electrolyte under AM 1.5 G 100 mW cm^{-2} simulated sunlight.

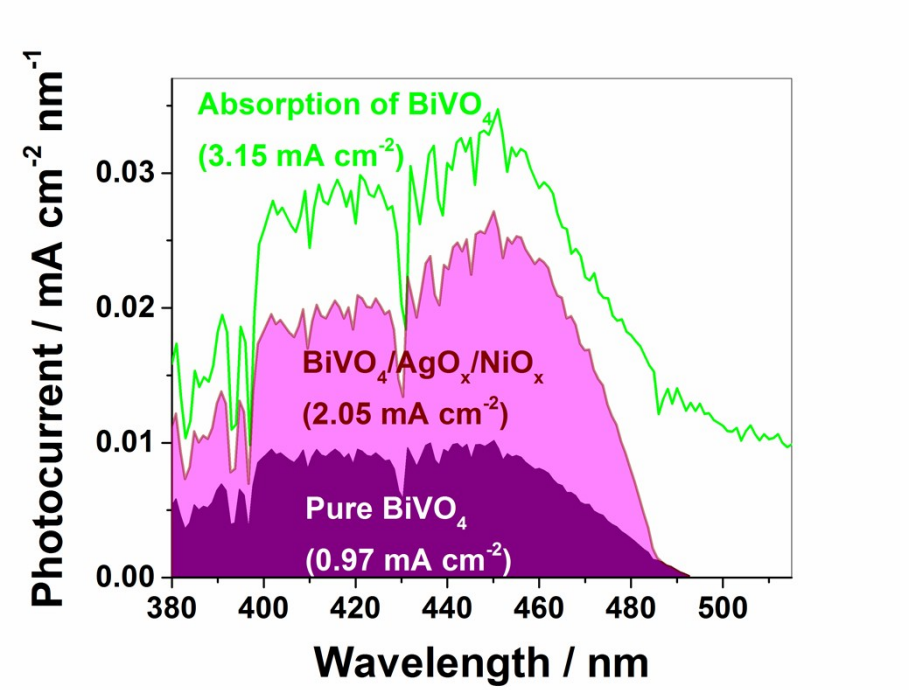

Fig. S6 Theoretical maximum photocurrent of the $BiVO_4$ (~ 95 nm) photoanode depended by the AM 1.5G 100 mW cm^{-2} solar spectrum; the integration of solar photocurrent spectra calculated from the AM 1.5G 100 mW cm^{-2} solar spectrum and the IPCE values.

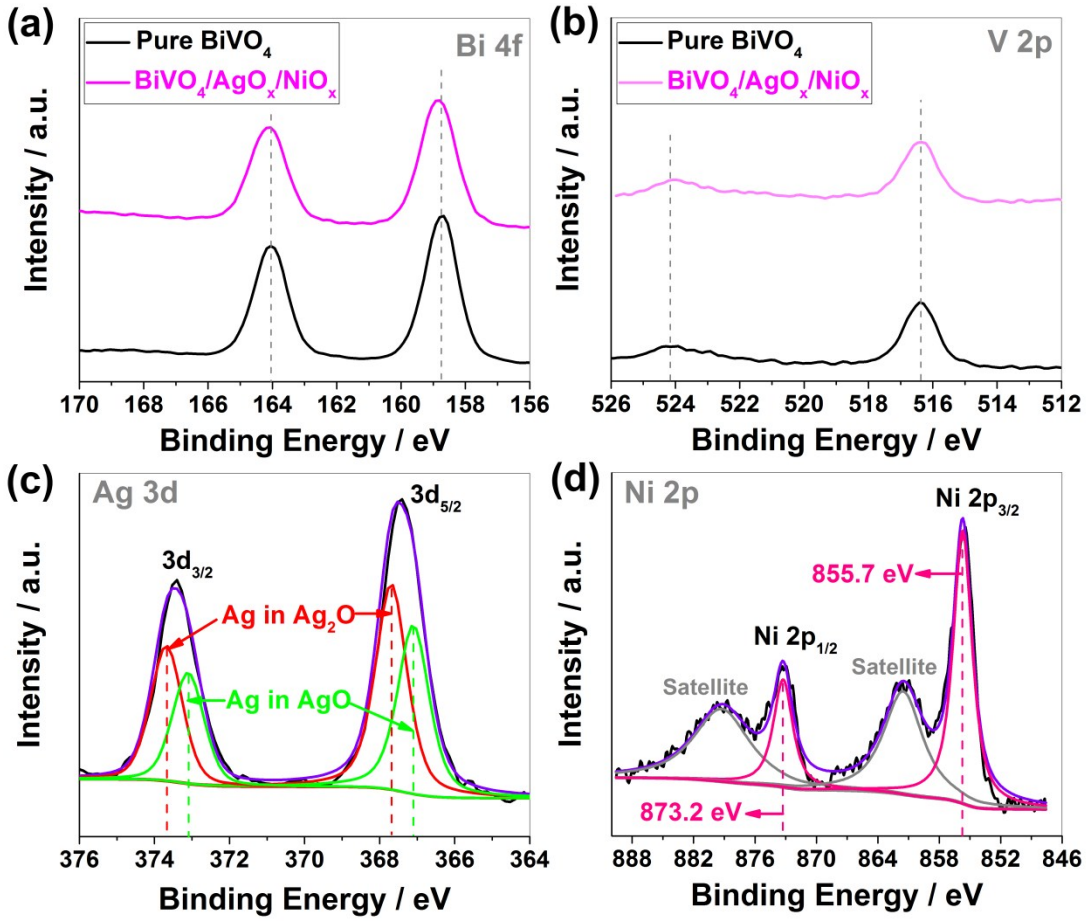

Fig. S7 XPS spectra of (a) Bi 4f and (b) V 2p in the pure $BiVO_4$ and $BiVO_4/AgO_x/NiO_x$ samples; (c) 3d electron spin-orbit of Ag and (d) 2p electron spin-orbit of Ni for the $BiVO_4/AgO_x/NiO_x$ sample.

The $BiVO_4$ and $BiVO_4/AgO_x/NiO_x$ films were analyzed by XPS to detect the actual composition and chemical states (Fig. S7). For pure $BiVO_4$, the V bands ($2p_{1/2}$ at 524.0 eV and $2p_{3/2}$ at 516.5 eV) and Bi bands ($4f_{5/2}$ at 164.0 eV and $4f_{7/2}$ at 158.7 eV) indicate that V is pentavalent and Bi is trivalent. The position of V and Bi bands remains the same demonstrating that $BiVO_4$ film loaded AgO_x and NiO_x maintains the original properties. For $BiVO_4/AgO_x/NiO_x$ sample, the binding energies of 367.1 eV ($3d_{5/2}$) and 373.1 eV ($3d_{3/2}$) are assigned to Ag(II), meanwhile, the binding energies of 367.7 eV ($3d_{5/2}$) and 373.7 eV ($3d_{3/2}$) match Ag(I), according to the previous reported data. This phenomenon means the chemical

state of silver includes both bivalent and monovalent. The Ni 2p spectrum in Fig. S7c shows two major peaks at 855.7 eV ($2p_{3/2}$) and 873.2 eV ($2p_{1/2}$) and two 2p satellite peaks, indicating the existence of Ni(II).

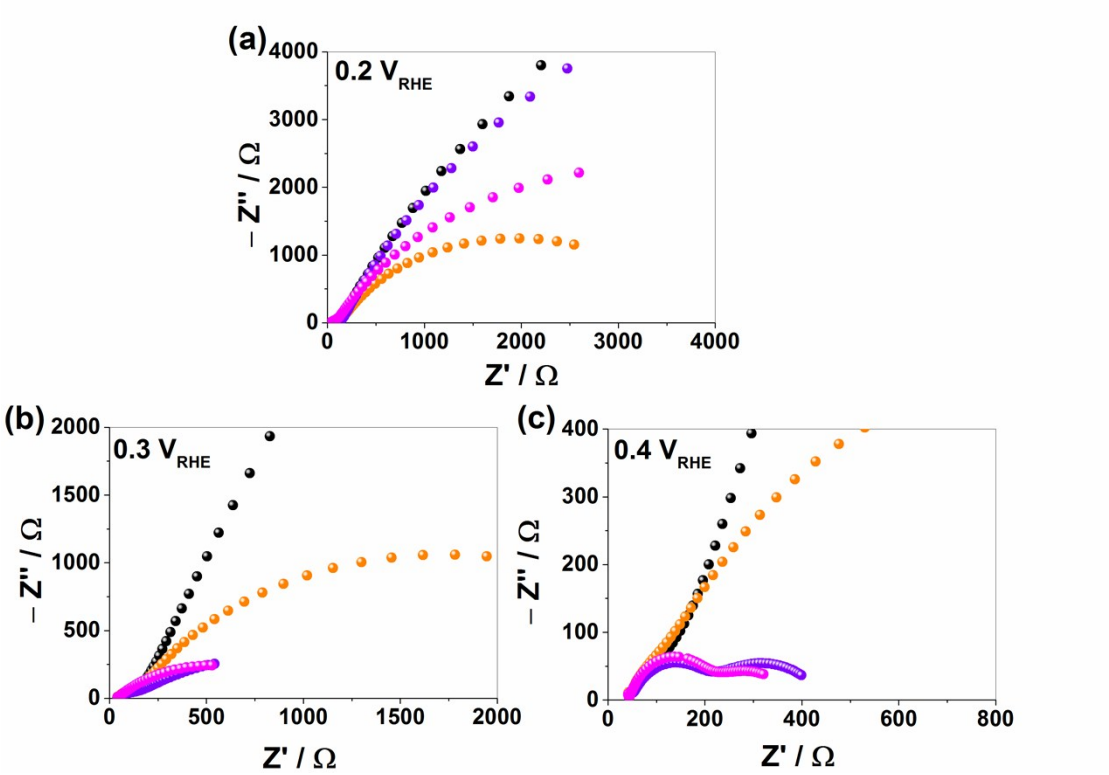

Fig. S8 Nyquist plots of the pure $BiVO_4$, $BiVO_4/AgO_x$, $BiVO_4/NiO_x$, and $BiVO_4/AgO_x/NiO_x$ photoanodes at various voltages, (a) 0.2 V_{RHE} ,(b) 0.3 V_{RHE}, and (c) 0.4 V_{RHE}. The photoanodes were irradiated in these EIS measurements.

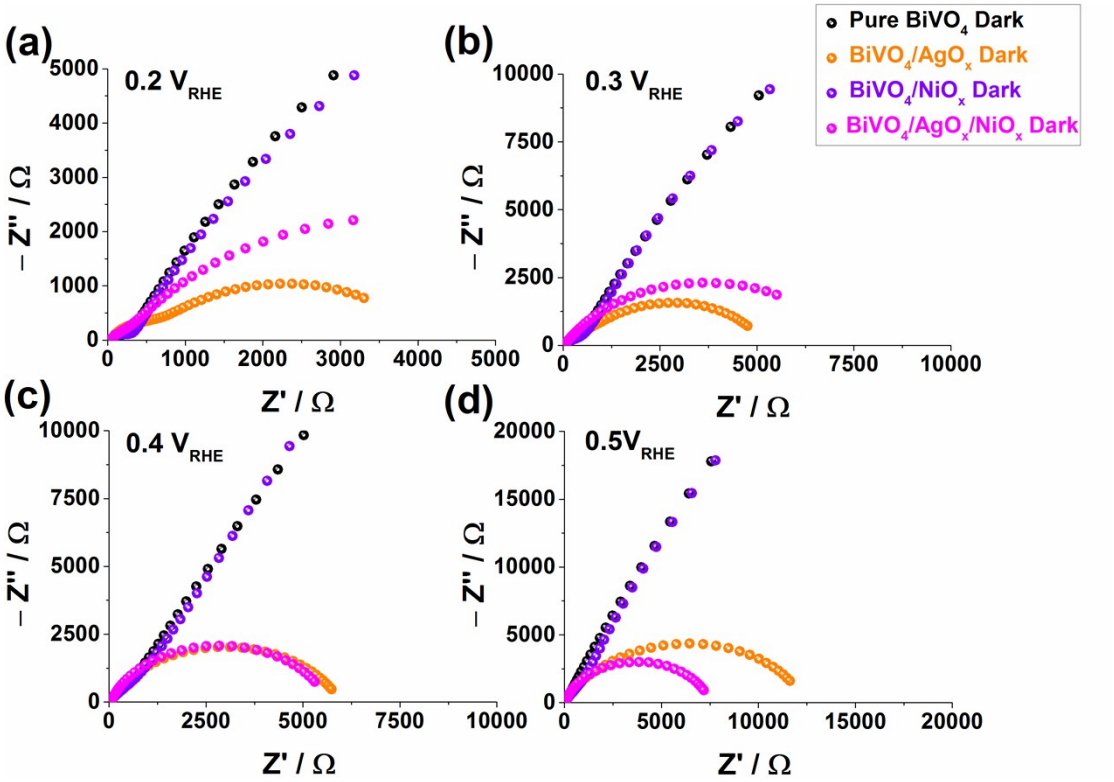

Fig. S9 Nyquist plots of all the samples at (a) 0.2 V_{RHE}, (b) 0.3 V_{RHE}, (c) 0.4 V_{RHE} and (d) 0.5 V_{RHE}.

The EIS measurements were executed in dark.

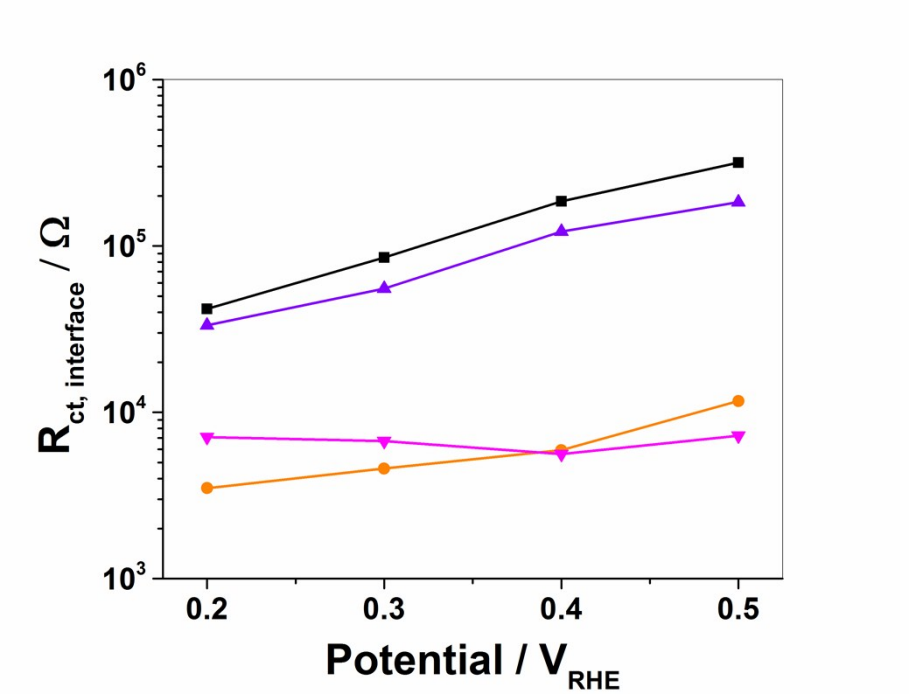

Fig. S10 Fitting values of $R_{ct,interface}$ (at 0.2—0.5 V_{RHE}) extracted from Nyquist plots (in dark) for the pure $BiVO_4$ (black), $BiVO_4/AgO_x$ (orange), $BiVO_4/NiO_x$ (violet), and $BiVO_4/AgO_x/NiO_x$ (magenta) photoanodes.

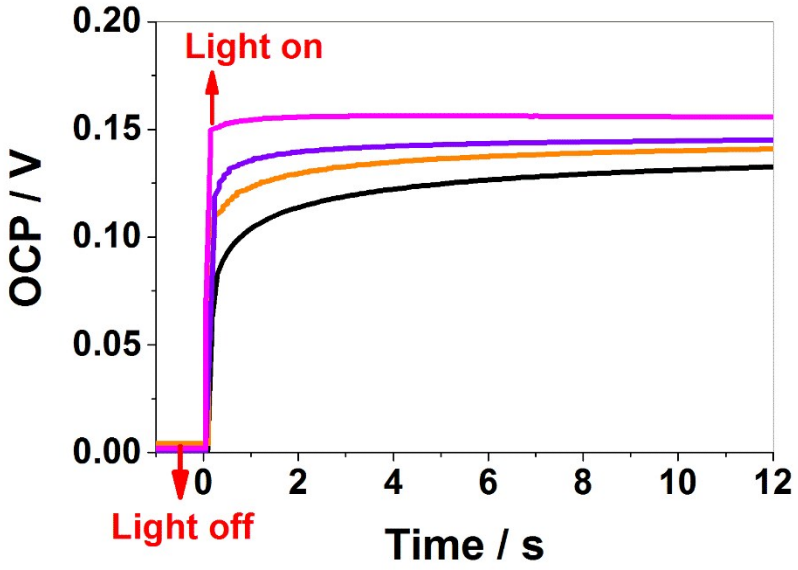

Fig. S11 Rise period of OCP values for the pure $BiVO_4$ (black), $BiVO_4/AgO_x$ (orange), $BiVO_4/NiO_x$ (violet), and $BiVO_4/AgO_x/NiO_x$ (magenta) photoanodes.

.

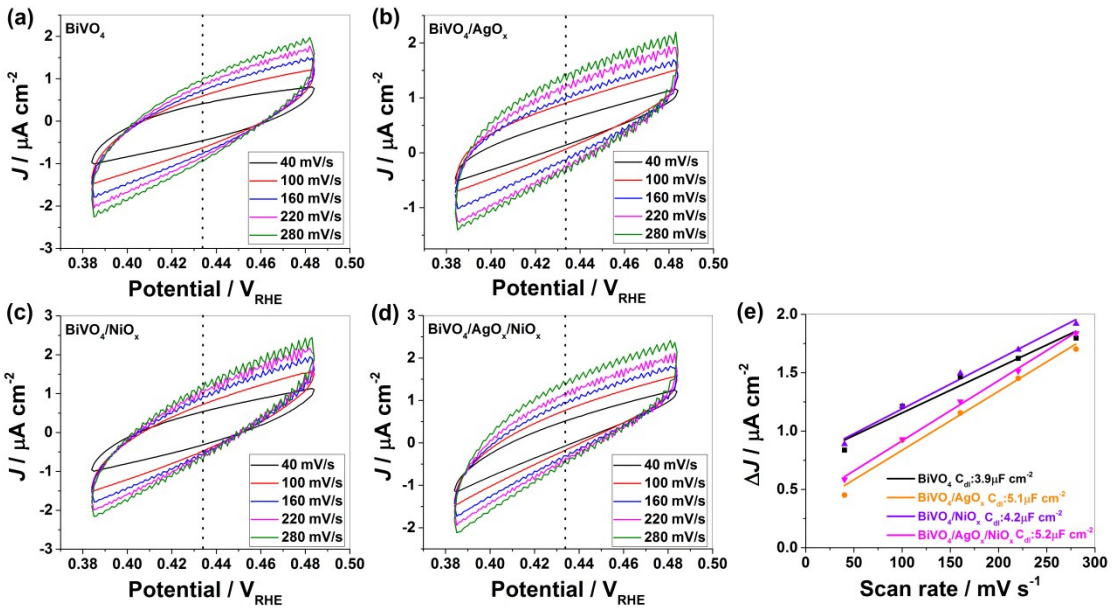

Fig. S12 Electrochemically active surface areas (ECSAs) measurements: cyclic voltammetry (CV) (CV) curves of the pure $BiVO_4$ (a), $BiVO_4/AgO_x$ (b), $BiVO_4/NiO_x$ (c), and $BiVO_4/AgO_x/NiO_x$ (d) photoanodes by various scan rates (40—280 mV/s); (e) double-layer capacitance (C_{dl}) depended by the difference between J_a and J_c values. The estimated electrochemically active surface areas of electrocatalysts are similar in the $BiVO_4$/OEC(s) systems.